

## Role of backflow correlations for the nonmagnetic phase of the $t-t'$ Hubbard model

Luca F. Tocchio,<sup>1,2</sup> Federico Becca,<sup>1,2</sup> Alberto Parola,<sup>3</sup> and Sandro Sorella<sup>1,2</sup>

<sup>1</sup>International School for Advanced Studies (SISSA), Via Beirut 2, I-34014 Trieste, Italy

<sup>2</sup>CNR-INFN-Democritos National Simulation Centre, Trieste, Italy

<sup>3</sup>Dipartimento di Fisica e Matematica, Università dell'Insubria, Via Valleggio 11, I-22100 Como, Italy

(Received 10 May 2008; revised manuscript received 11 June 2008; published 7 July 2008)

We introduce an efficient way to improve the accuracy of projected wave functions, widely used to study the two-dimensional Hubbard model. Taking the clue from the backflow contribution, whose relevance has been emphasized for various interacting systems on the continuum, we consider many-body correlations to construct a suitable approximation for the ground state at intermediate and strong couplings. In particular, we study the phase diagram of the frustrated  $t-t'$  Hubbard model on the square lattice and show that, thanks to backflow correlations, an insulating and nonmagnetic phase can be stabilized at strong coupling and sufficiently large frustrating ratio  $t'/t$ .

DOI: 10.1103/PhysRevB.78.041101

PACS number(s): 71.10.Fd, 71.27.+a, 71.30.+h, 75.10.-b

### I. INTRODUCTION

Recently, the interest in the role of frustrating interactions in electronic systems has considerably increased, since in this regime new exotic phases may appear. Many experiments suggest the possibility to have disordered phases down to very low temperatures (much smaller than what one would expect from a mean-field approach) or even to zero temperature. Such phases are generically called spin liquids. In this respect, the organic molecular materials  $\kappa$ -(ET)<sub>2</sub>X, X being a monovalent anion,<sup>1,2</sup> represent an interesting example, since they show a particularly rich phase diagram. In the conducting layers, ET molecules are strongly dimerized and form a two-dimensional (2D) triangular lattice. Since the valence of each ET dimer is +1, the conduction band is half filled. By acting with an external pressure, it is possible to vary the ratio between the on-site Coulomb repulsion and the bandwidth, driving the system through a metal-insulator transition.

The minimal model to describe the physics of correlated electrons is the Hubbard model

$$\mathcal{H} = - \sum_{i,j,\sigma} t_{ij} c_{i,\sigma}^\dagger c_{j,\sigma} + \text{H.c.} + U \sum_i n_{i,\uparrow} n_{i,\downarrow}, \quad (1)$$

where  $c_{i,\sigma}^\dagger$  ( $c_{i,\sigma}$ ) creates (destroys) an electron with spin  $\sigma$  on site  $i$ ,  $n_{i,\sigma} = c_{i,\sigma}^\dagger c_{i,\sigma}$ ,  $t_{ij}$  is the hopping amplitude that determines the bandwidth, and  $U$  is the on-site Coulomb repulsion. In this work, we focus our attention on the half-filled case with  $N$  electrons on  $N$  sites (tilted by  $45^\circ$ ), and consider the square lattice with both nearest- and next-nearest-neighbor hoppings, denoted by  $t$  and  $t'$ , respectively. This model represents the prototype for frustrated electronic materials,<sup>3</sup> and, recently, it has been widely studied by different numerical techniques, with contradictory outcomes.<sup>4-8</sup> Here, we present the results for the zero-temperature phase diagram, obtained by using projected wave functions.

### II. VARIATIONAL APPROACH

Variational wave functions for the unfrustrated Hubbard model, describing the antiferromagnetic phase, can be con-

structed by considering the ground state  $|AF\rangle$  of a mean-field Hamiltonian containing a band contribution and a magnetic term  $\mathcal{H}_{AF} = \Delta_{AF} \sum_j e^{i\mathbf{Q}\cdot\mathbf{R}_j} S_j^x$ , where  $S_j^x$  is the  $x$  component of the spin operator  $\mathbf{S}_j = (S_j^x, S_j^y, S_j^z)$ . In order to have the correct spin-spin correlations at large distance, we have to apply a suitable long-range spin Jastrow factor, namely,  $|\Psi_{AF}\rangle = \mathcal{J}_s |AF\rangle$ , with  $\mathcal{J}_s = \exp[-\frac{1}{2} \sum_{i,j} \mu_{i,j} S_i^z S_j^z]$ , which governs spin fluctuations orthogonal to the magnetic field  $\Delta_{AF}$ .<sup>9</sup>

On the other hand, spin-liquid (i.e., disordered) states can be constructed by considering the ground state  $|BCS\rangle$  of a Bardeen-Cooper-Schrieffer (BCS) Hamiltonian and then applying to it the so-called Gutzwiller projector,  $|RVB\rangle = \mathcal{P}_G |BCS\rangle$ , where  $\mathcal{P}_G = \prod_i (1 - g n_{i,\uparrow} n_{i,\downarrow})$  and  $g = 1$ .<sup>10,11</sup> In pure spin models, where the  $U$  is infinite and charge fluctuations are completely frozen, these kinds of states can be remarkably accurate and provide important predictions on the stabilization of disordered spin-liquid ground states.<sup>12,13</sup> However, whenever  $U/t$  is finite, the variational state must also contain charge fluctuations. In this regard, the simplest generalization of the Gutzwiller projector with  $g < 1$ , which allows doubly occupied sites, is known to lead to a metallic phase.<sup>14</sup> In order to obtain a Mott insulator with no magnetic order, it is necessary to consider a sufficiently long-range Jastrow factor  $\mathcal{J} = \exp[-\frac{1}{2} \sum_{i,j} v_{i,j} n_i n_j]$ ,  $n_i = \sum_\sigma n_{i,\sigma}$  being the local density.<sup>15</sup> Nevertheless, the accuracy of the resulting wave function  $|\Psi_{BCS}\rangle = \mathcal{J} |BCS\rangle$  can be rather poor in 2D for large on-site interactions,<sup>16</sup> especially in the presence of frustration (see below). Therefore, other contributions beyond the Jastrow factor must be included. In this respect, some improvement on small clusters can be also obtained by performing one Lanczos step,  $(1 + \alpha \mathcal{H}) |\Psi_{BCS}\rangle$ ,<sup>9</sup> or by considering  $\exp(hK) \mathcal{P}_G |BCS\rangle$  (where  $h$  and  $g$  are variational parameters and  $K$  is the hopping Hamiltonian).<sup>17</sup> However, the first case is clearly not size consistent, while the second one becomes highly inefficient on large clusters.

### III. BACKFLOW WAVE FUNCTION

The poor accuracy of  $|\Psi_{BCS}\rangle$  is particularly evident in the strong-coupling limit, where the super-exchange-energy

scale is not correctly reproduced. Here, we want to modify the single-particle orbitals<sup>18</sup> in the same spirit of the backflow correlations, which have been proposed a long time ago by Feynman and Cohen<sup>19</sup> to obtain a quantitative description of the roton excitation in liquid Helium. In our context, the backflow term makes it possible to mimic the effect of the virtual hopping, which leads to the super-exchange mechanism. In the following, we will show that backflow correlations will be particularly important for the BCS wave function, whereas they are less crucial in all magnetically ordered phases, where already the mean-field state can satisfy the single-occupancy (strong-coupling) constraint and contains the virtual hopping processes, which are generated by the kinetic term.

The backflow has been implemented within quantum Monte Carlo calculations to study bulk liquid <sup>3</sup>He,<sup>20,21</sup> and used to improve the description of the electron jellium both in two and three dimensions.<sup>22,23</sup> More recently, it has been applied to metallic hydrogen.<sup>24</sup> Originally, the backflow term corresponds to consider fictitious coordinates of the electrons  $\mathbf{r}_\alpha^b$ , which depend on the positions of the other particles, so to create a return flow of current,

$$\mathbf{r}_\alpha^b = \mathbf{r}_\alpha + \sum_\beta \eta_{\alpha,\beta}[x](\mathbf{r}_\beta - \mathbf{r}_\alpha), \quad (2)$$

where  $\mathbf{r}_\alpha$  are the actual electronic positions and  $\eta_{\alpha,\beta}[x]$  are variational parameters depending in principle on all the electronic coordinates, namely, on the many-body configuration  $|x\rangle$ . The variational wave function is then constructed by means of the orbitals calculated in the new positions, i.e.,  $\phi(\mathbf{r}_\alpha^b)$ . Alternatively, the backflow can be introduced by considering a linear expansion of each single-particle orbital:

$$\phi_k(\mathbf{r}_\alpha^b) \approx \phi_k^b(\mathbf{r}_\alpha) \equiv \phi_k(\mathbf{r}_\alpha) + \sum_\beta c_{\alpha,\beta}[x]\phi_k(\mathbf{r}_\beta), \quad (3)$$

where  $c_{\alpha,\beta}[x]$  are suitable coefficients. Definition (3) is particularly useful in lattice models, where the coordinates of the particles may assume only discrete values. In particular, in the Hubbard model, the form of the new ‘‘orbitals’’ can be fixed by considering the  $U \gg t$  limit, so to favor a recombination of neighboring charge fluctuations (i.e., empty and doubly-occupied sites),

$$\phi_k^b(\mathbf{r}_{i,\sigma}) \equiv \epsilon\phi_k(\mathbf{r}_{i,\sigma}) + \eta \sum_j t_{ij}(D_i H_j)\phi_k(\mathbf{r}_{j,\sigma}), \quad (4)$$

where we used the notation that  $\phi_k(\mathbf{r}_{i,\sigma}) = \langle 0 | c_{i,\sigma} | \phi_k \rangle$ ,  $|\phi_k\rangle$  are the eigenstates of the mean-field Hamiltonian,  $D_i = n_{i,\uparrow} n_{i,\downarrow}$ , and  $H_i = h_{i,\uparrow} h_{i,\downarrow}$ , with  $h_{i,\sigma} = (1 - n_{i,\sigma})$ , so that  $D_i$  and  $H_i$  are nonzero only if the site  $i$  is doubly occupied or empty, respectively; finally  $\epsilon$  and  $\eta$  are variational parameters (we can assume that  $\epsilon = 1$  if  $D_i H_j = 0$ ). As a consequence, the determinant part of the wave function already includes correlation effects due to the presence of the many-body operator  $D_i H_j$ . The previous definition of the backflow term preserves the spin SU(2) symmetry. A further generalization of the new ‘‘orbitals’’ can be made by taking all the possible virtual hoppings of the electrons:

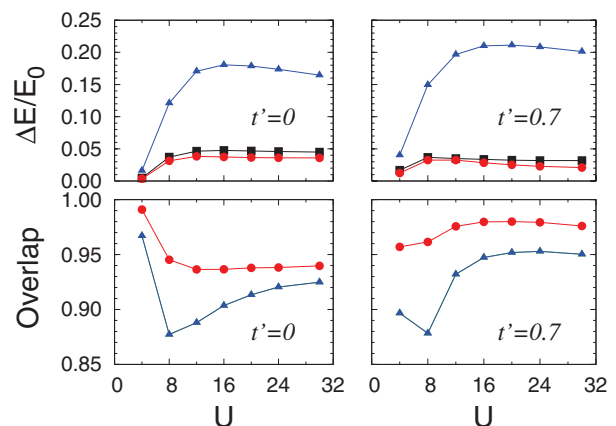


FIG. 1. (Color online) Results for 18 electrons on 18 sites as a function of  $U/t$ . Upper panels: Accuracy of energy  $\Delta E = (E_0 - E_v)$ ,  $E_v$ , and  $E_0$  being the variational and the exact values, respectively. Lower panels: Overlap between the exact ground state and the variational wave functions. The BCS state with long-range Jastrow factor is denoted by blue triangles, the BCS state with backflow correlations and Jastrow term by red circles. The results for  $\Delta E$  considering one Lanczos step upon the BCS state, i.e.,  $(1 + \alpha\mathcal{H})|\Psi\rangle$ , are also shown (black squares).

$$\begin{aligned} \phi_k^b(\mathbf{r}_{i,\sigma}) \equiv & \epsilon\phi_k(\mathbf{r}_{i,\sigma}) + \eta_1 \sum_j t_{ij}(D_i H_j)\phi_k(\mathbf{r}_{j,\sigma}) \\ & + \eta_2 \sum_j t_{ij}(n_{i,\sigma} h_{i,-\sigma} n_{j,-\sigma} h_{j,\sigma})\phi_k(\mathbf{r}_{j,\sigma}) \\ & + \eta_3 \sum_j t_{ij}(D_i n_{j,-\sigma} h_{j,\sigma} + n_{i,\sigma} h_{i,-\sigma} H_j)\phi_k(\mathbf{r}_{j,\sigma}), \end{aligned} \quad (5)$$

where  $\epsilon$ ,  $\eta_1$ ,  $\eta_2$ , and  $\eta_3$  are variational parameters. The latter two variational parameters are particularly important for the metallic phase at small  $U/t$ , whereas they give only a slight improvement of the variational wave function in the insulator at strong coupling. For simplicity, we take the same parameters for up and down electrons. The definition Eq. (5) may break the SU(2) symmetry, however, the optimized wave function always has a very small value of the total spin square, i.e.,  $\langle S^2 \rangle \sim 0.001$  for 50 sites. All the parameters of the wave function (contained in the mean-field Hamiltonian, in the Jastrow term, and in the backflow term) can be optimized by using the method of Ref. 13. Finally, the variational results can be compared to more accurate (and still variational) ones obtained by Green’s function Monte Carlo implemented with the so-called fixed-node (FN) approximation.<sup>25</sup>

#### IV. RESULTS

Let us start by considering the comparison of the variational results with the exact ones on the 18-site cluster at half filling. In Fig. 1, we show the accuracy of the variational BCS state (with and without backflow correlations) and the overlap with the exact ground state for two values of the frustrating ratio, i.e.,  $t'/t = 0$  and 0.7. The backflow term is

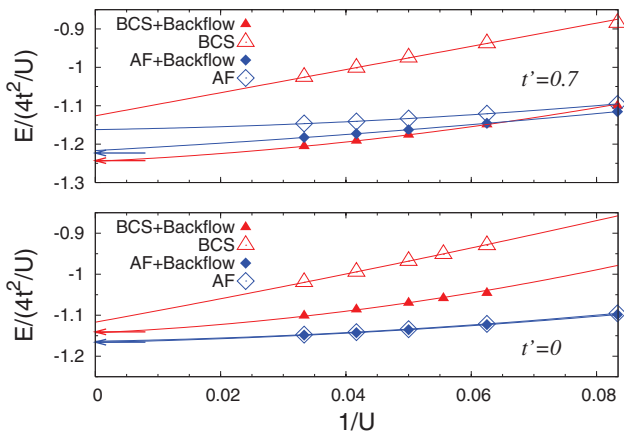


FIG. 2. (Color online) Variational energies per site (in unit of  $J=4t^2/U$ ) for the BCS state with a Jastrow factor, with and without backflow correlations, and 98 sites. The results for the wave function with antiferromagnetic order and no BCS pairing are also shown. Arrows indicate the variational results obtained by applying the full Gutzwiller projection to the mean-field states for the corresponding Heisenberg models.

able to highly improve the accuracy both for weak and strong couplings. We also notice that backflow correlations are more efficient than applying one Lanczos step, i.e.,  $(1+\alpha\mathcal{H})|\Psi_{\text{BCS}}\rangle$ , which was used in previous calculations.<sup>9</sup> The overlap between the exact ground state and the backflow state remains very high even for large  $U$ , especially in the frustrated regime.

Backflow correlations remain efficient also for larger sizes and provide much lower energy than the Lanczos step wave function, e.g., for 98 sites with  $U/t=20$  and  $t'/t=0.7$ , the energy per site with the backflow wave function is  $E_b/t = -0.2352(1)$ , while the one with one Lanczos step is  $E_{ls}/t = -0.2310(1)$  (for 18 sites they are  $E_b/t = -0.23741$  and  $E_{ls}/t = -0.23566$ ). The FN energy obtained with the backflow state is  $E_{\text{FN}}/t = -0.2395(1)$ , rather close to our estimation of the exact value (based upon an extrapolation obtained with zero and one Lanczos step) that is  $E/t \sim -0.246$ .

By increasing  $U/t$ , the variational energy extrapolates to the one obtained by taking the fully projected state  $|RVB\rangle$  in the spin model. On the contrary, without using backflow terms, the energy of the BCS state, even in the presence of a fully optimized Jastrow factor, is few hundredths of  $J=4t^2/U$  higher than the expected value (see Fig. 2). Moreover, whenever frustration is large enough, backflow correlations are also useful in the antiferromagnetic state  $|\Psi_{\text{AF}}\rangle$ , while for  $t'/t=0$  they are not necessary to extrapolate to the value of the spin model (see Fig. 2).

In order to draw the ground-state phase diagram of the  $t-t'$  Hubbard model, we consider three different wave functions with backflow correlations: Two antiferromagnetic states  $|\Psi_{\text{AF}}\rangle$  with  $\mathbf{Q}=(\pi, \pi)$  and  $\mathbf{Q}=(\pi, 0)$ , relevant for small and large  $t'/t$ , and the nonmagnetic state  $|\Psi_{\text{BCS}}\rangle$ . The variational phase diagram is reported in Fig. 3. The first important outcome is that without backflow terms, the energies of the spin-liquid wave function are *always* higher than those of the magnetically ordered states for any value of frustration  $t'/t$ .

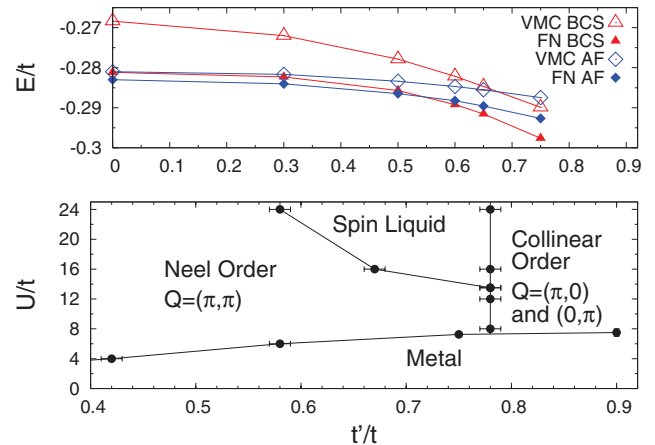


FIG. 3. (Color online) Lower panel: Phase diagram of the frustrated  $t-t'$  Hubbard model as obtained by comparing the variational energies of the backflow wave functions. Upper panel: Comparison between the variational (VMC) energies per site (with backflow correlations) and the FN ones for  $U/t=16$  and 98 sites.

Instead, by inserting backflow correlations, a spin-liquid phase can be stabilized at large enough  $U/t$  and frustration (see also Fig. 2). The small energy difference between the pure variational and the FN energies demonstrates the accuracy of the backflow states, see Fig. 3. Notice that  $|\Psi_{\text{AF}}\rangle$  and  $|\Psi_{\text{BCS}}\rangle$  have different nodal surfaces, implying different FN energies.

For small Coulomb repulsion and finite  $t'/t$  the static density-density correlations  $N(q)=\langle n_{-q}n_q \rangle$  (where  $n_q$  is the Fourier transform of the local density  $n_i$ ) have a linear behavior for  $|q|\rightarrow 0$ , typical of a conducting phase. A very small superconducting parameter with  $d_{x^2-y^2}$  symmetry can be stabilized, suggesting that long-range pairing correlations, if any, are tiny. By increasing  $U/t$ , a metal-insulator transition is found and  $N(q)$  acquires a quadratic behavior in the insulating phase, indicating a vanishing compressibility. This behavior does not change when considering the FN approach, although the metal-insulator transition may be slightly shifted. In Fig. 4, we show the variational results for  $N(q)$  as a function of  $U/t$  for  $t'/t=0.75$ . The insulator just above the transition is magnetically ordered and the variational wave function has a large  $\Delta_{\text{AF}}$ ; the transition is likely to be first order. By further increasing  $U/t$ , there is a second transition to a disordered insulator. Indeed, for  $U/t \geq 14$ , the energy of the BCS wave function becomes lower than the one of the antiferromagnetic state. In this respect, the key ingredient to have such an insulating behavior is the presence of a singular Jastrow term  $v_q \sim 1/q^2$ , which turns a BCS superconductor into a Mott insulator.<sup>15</sup> In contrast to previous investigations,<sup>4-8</sup> for intermediate on-site couplings, our calculations indicate the possibility to have a direct (first-order) transition between two magnetic states (see Fig. 3).

In order to verify the magnetic properties obtained within the variational approach, we can consider the static spin-spin correlations  $S(q)=\langle S_{-q}^z S_q^z \rangle$  over the FN ground state. Although the FN approach may break the  $SU(2)$  spin symmetry, favoring a spin alignment along the  $z$  axis (this is what we find for small lattices by a direct comparison with exact

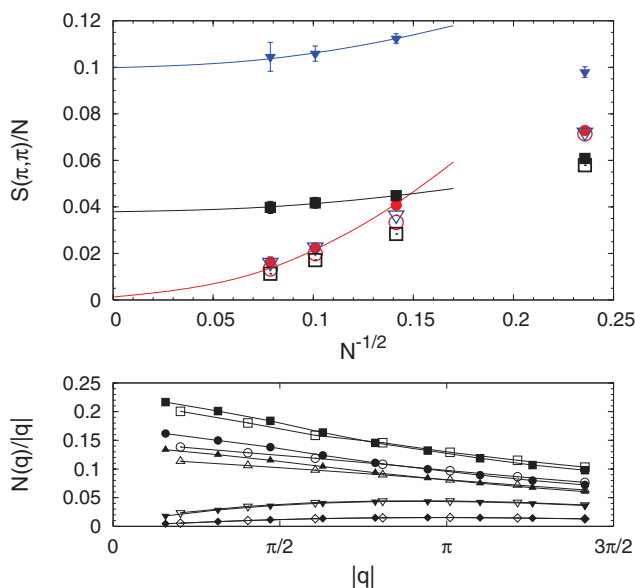


FIG. 4. (Color online) Upper panel: Variational (empty symbols) and FN (full symbols) results for  $S(\pi, \pi)$  divided by  $N$ . Both calculations have been done by using the projected BCS wave function;  $U/t=16$  and  $t'/t=0$  (triangles),  $U/t=24$  and  $t'/t=0.7$  (circles), and  $U/t=8$  and  $t'/t=0.75$  (squares). Lines are guides to the eye. Lower panel: Variational results for  $N(q)$  divided by  $|q|$  for 98 (empty symbols) and 162 (full symbols) sites and  $t'/t=0.75$ ; from top to bottom:  $U/t=4, 6, 7, 8,$  and  $16$ .

results),  $S(q)$  is particularly simple to evaluate within this approach,<sup>25</sup> and it gives important insights into the magnetic properties of the ground state. In Fig. 4, we report the comparison between the variational and the FN results by considering the nonmagnetic state  $|\Psi_{\text{BCS}}\rangle$ . Remarkably, in the unfrustrated case, where antiferromagnetic order is expected, the FN approach is able to increase spin-spin correlations at  $q=(\pi, \pi)$ , even by considering the nonmagnetic wave function to fix the nodes. A finite value of the magnetization is also plausible in the insulating region just above the metallic phase at strong frustration (i.e.,  $t'/t \sim 0.75$ ), confirming the variational calculations. On the contrary, by increasing the electron correlation, the FN results change only slightly the variational value of  $S(\pi, \pi)$ , indicating the stability of the disordered state. In this case, a qualitatively correct representation of the ground state is obtained by the simple  $|\Psi_{\text{BCS}}\rangle$ .

In conclusion, we have introduced a wave function that highly improves the accuracy of the projected states used so far. Our variational ansatz is particularly useful to describe nonmagnetic phases, which can be stabilized in the strong-coupling regime of the  $t-t'$  Hubbard model on the square lattice.

#### ACKNOWLEDGMENT

We acknowledge partial support from CNR-INFM.

- <sup>1</sup>Y. Shimizu, K. Miyagawa, K. Kanoda, M. Maesato, and G. Saito, Phys. Rev. Lett. **91**, 107001 (2003).
- <sup>2</sup>Y. Kurosaki, Y. Shimizu, K. Miyagawa, K. Kanoda, and G. Saito, Phys. Rev. Lett. **95**, 177001 (2005).
- <sup>3</sup>H. Q. Lin and J. E. Hirsch, Phys. Rev. B **35**, 3359 (1987).
- <sup>4</sup>T. Kashima and M. Imada, J. Phys. Soc. Jpn. **70**, 3052 (2001).
- <sup>5</sup>H. Morita, S. Watanabe, and M. Imada, J. Phys. Soc. Jpn. **71**, 2109 (2002).
- <sup>6</sup>T. Mizusaki and M. Imada, Phys. Rev. B **74**, 014421 (2006).
- <sup>7</sup>H. Yokoyama, M. Ogata, and Y. Tanaka, J. Phys. Soc. Jpn. **75**, 114706 (2006).
- <sup>8</sup>A. H. Nevidomskyy, C. Scheiber, D. Senechal, and A.-M. S. Tremblay, Phys. Rev. B **77**, 064427 (2008); see also, S. R. Hassan, B. Davoudi, B. Kyung, and A.-M. S. Tremblay, *ibid.* **77**, 094501 (2008).
- <sup>9</sup>F. Becca, M. Capone, and S. Sorella, Phys. Rev. B **62**, 12700 (2000).
- <sup>10</sup>P. W. Anderson, Science **235**, 1196 (1987).
- <sup>11</sup>B. Edegger, V. N. Muthukumar, and C. Gros, Adv. Phys. **56**, 927 (2007).
- <sup>12</sup>L. Capriotti, F. Becca, A. Parola, and S. Sorella, Phys. Rev. Lett. **87**, 097201 (2001).
- <sup>13</sup>S. Yunoki and S. Sorella, Phys. Rev. B **74**, 014408 (2006).
- <sup>14</sup>H. Yokoyama and H. Shiba, J. Phys. Soc. Jpn. **56**, 1490 (1987).
- <sup>15</sup>M. Capello, F. Becca, M. Fabrizio, S. Sorella, and E. Tosatti, Phys. Rev. Lett. **94**, 026406 (2005).
- <sup>16</sup>M. Capello, Ph.D. thesis (SISSA, Trieste).
- <sup>17</sup>D. Eichenberger and D. Baeriswyl, Phys. Rev. B **76**, 180504(R) (2007).
- <sup>18</sup>After the particle-hole transformation on down spins  $c_{i,\downarrow}^\dagger \rightarrow c_{i,\downarrow}$ , the BCS Hamiltonian conserves the particle number and it is possible to define single-particle states.
- <sup>19</sup>R. P. Feynman and M. Cohen, Phys. Rev. **102**, 1189 (1956).
- <sup>20</sup>M. A. Lee, K. E. Schmidt, M. H. Kalos, and G. V. Chester, Phys. Rev. Lett. **46**, 728 (1981).
- <sup>21</sup>K. E. Schmidt, M. A. Lee, M. H. Kalos, and G. V. Chester, Phys. Rev. Lett. **47**, 807 (1981).
- <sup>22</sup>Y. Kwon, D. M. Ceperley, and R. M. Martin, Phys. Rev. B **48**, 12037 (1993).
- <sup>23</sup>Y. Kwon, D. M. Ceperley, and R. M. Martin, Phys. Rev. B **58**, 6800 (1998).
- <sup>24</sup>M. Holzmann, D. M. Ceperley, C. Pierleoni, and K. Esler, Phys. Rev. E **68**, 046707 (2003).
- <sup>25</sup>D. F. B. ten Haaf, H. J. M. van Bommel, J. M. J. van Leeuwen, W. van Saarloos, and D. M. Ceperley, Phys. Rev. B **51**, 13039 (1995).